



Optical Bistability and Normal-Mode Splitting of Two-Species Bose-Einstein Condensates in An Optical Cavity

Research Article

Neha Aggarwal¹, Shweta², Aranya B. Bhattacharjee³ and Man Mohan¹

¹ Department of Physics and Astrophysics, University of Delhi, Delhi 110007, India

² School of Basic and Applied Sciences, Department of Physics, Galgotias University, Greater Noida, Uttar Pradesh 201306, India

³ School of Physical Sciences, Jawaharlal Nehru University, New Delhi 110067, India

*Corresponding author: ag.neha88@gmail.com

Abstract. We investigate the optical bistable behavior for a weakly interacting two-species Bose-Einstein condensates inside a pumped optical cavity by considering the two possible regimes – the phase mixed regime and the phase segregated regime. We find that the cavity-pump detuning plays a significant role in controlling the threshold of the optical bistability and the contrast between the bistability values depending upon the state we are working in. We also demonstrate the occurrence of normal mode splitting in the optical spectrum for both the regimes which further showing the position and amplitude discrepancies in the spectral peaks.

Keywords. Two-species Bose-Einstein condensates; Optical bistability; Normal-mode splitting

PACS. 03.75.Mn; 03.75.Kk; 37.30.+i; 42.65.Pc

Received: July 30, 2015

Accepted: August 27, 2015

Copyright © 2015 Neha Aggarwal, Shweta, Aranya B. Bhattacharjee and Man Mohan. *This is an open access article distributed under the Creative Commons Attribution License, which permits unrestricted use, distribution, and reproduction in any medium, provided the original work is properly cited.*

1. Introduction

Ultracold atomic ensembles confined in a small volume ultrahigh-finesse optical cavity have always been studied for the past many years from many different points of view. Such system forms a very nice example of a nonlinear system. When the resonance frequency of the cavity is far detuned from the atomic resonance, the nonlinearity in the system arises due to the

dispersive interaction between the light and the atom. This atom-light interaction imprints a position-dependent phase shift on the light field which in turn affects the mechanical motion of the atoms. This highly nonlocal nonlinear interaction is very different from the usual local interatomic interactions. Many interesting results have been reported by exploiting this nonlinear interaction such as optical bistability [1], self-organization of atoms [2], cavity-enhanced super-radiant Rayleigh scattering [3], Bose-Hubbard model [4] and Dicke quantum phase transition [5]. Furthermore, in recent years, Bose-Einstein condensates (BECs) in optical resonators and another important field of research i.e., optomechanics were unified where the collective motion of an atomic ensemble plays the role of movable mirror [6]. In 1980s, optical bistability was extensively studied due to the prospect of its use in all-optical computers as an optical switch [7]. However, there were limited applications due to the lack of controllability. Recently, the controlled optical bistability threshold points and width of bistability hysteresis curve have not only been studied theoretically but have also been observed experimentally [8, 9]. The BEC-cavity system also shows strong matter-wave bistability [10] and optical bistability [6, 11].

The aim of the present paper is to analyse optical bistability and normal-mode splitting for a two-species BECs confined within an optical cavity. Since the experimental realization of binary mixtures of Bose-Einstein condensates (BECs) in 1997 [12], the field of two-component BECs has always been an intense research topic both experimentally and theoretically. These have been experimentally achieved using different isotopes of the same atom [13], different atomic species [14–17], and two hyperfine states of the single isotope [12, 18–23]. Depending upon the atom-atom interaction strengths G_{ii} (intraspecies interactions) and $G_{ij}(i \neq j)$ (interspecies interaction), these binary mixtures can be either in a phase mixed state ($G_{12}^2 < G_{11}G_{22}$) or in a phase segregated state ($G_{12}^2 > G_{11}G_{22}$) [24]. The nonlinear interaction can be manipulated using Feshbach resonances very conveniently [25]. The purpose of the present paper is to investigate the influence of these atomic interactions on the optical bistability of the pumped two species BEC-cavity system. We further discuss how cavity-pump detuning plays a vital role in controlling the threshold points of the bistability depending upon the state the condensates are in. In addition, we also study the normal mode splitting in the displacement spectrum of the optical cavity field for both the phase mixed and phase segregated cases.

2. The Model Hamiltonian

We consider a zero-temperature two-species Bose-Einstein condensate system with weak nonlinear interatomic interaction strongly interacting with a quantized single standing wave cavity mode of frequency ω_c , whose schematic representation is shown in Figure 2. The cavity field is also coupled to external fields incident from one side mirror. In order to reduce the decoherence, the system can be isolated from the environment by using a high-Q optical cavity. This also ensures that the cavity light field remains quantum mechanical for the duration of the experiment. The single cavity mode approximation is justified if the induced resonance frequency shift of the cavity is much smaller than the longitudinal-mode spacing. The cavity is coherently driven by a laser field with frequency ω_p through the cavity mirror with amplitude η . The harmonic confinement along the direction perpendicular to the optical lattice is taken to

be large so that the system effectively reduces to one dimension. In the formalism of the second quantization, the Hamiltonian of such a system can be written as [26–28]:

$$H = H_0 + H_{int} + H_L, \quad (1)$$

where

$$H_0 = \sum_{i=1,2} \int d\vec{x} \psi_i^\dagger(\vec{x}) \left[-\frac{\hbar^2 \nabla^2}{2M} + V_i(\vec{x}) + \frac{4\pi\hbar^2 a_i}{2M} \psi_i^\dagger(\vec{x}) \psi_i(\vec{x}) \right] \psi_i(\vec{x}), \quad (2)$$

$$V_i(\vec{x}) = \cos^2(kx) [\hbar U_{0i} \hat{a}^\dagger \hat{a} + V_i^{cl}], \quad (3)$$

$$H_{int} = \frac{4\pi\hbar^2 a_{12}}{M} \int d\vec{x} \psi_1^\dagger(\vec{x}) \psi_2^\dagger(\vec{x}) \psi_1(\vec{x}) \psi_2(\vec{x}), \quad (4)$$

$$H_L = -\hbar\Delta_c \hat{a}^\dagger \hat{a} - i\hbar\eta(\hat{a} - \hat{a}^\dagger). \quad (5)$$

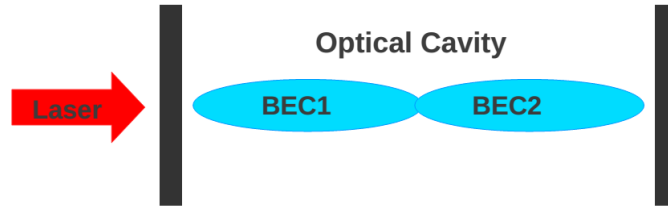


Figure 1. (color online) Schematic representation of the system we are investigating here. It involves the weakly interacting two-species Bose-Einstein condensates inside a Fabry-Perot optical cavity driven by an external pump laser.

The atomic creation and annihilation field operators of the i th condensate at position \vec{x} are represented by $\psi_i^\dagger(\vec{x})$ and $\psi_i(\vec{x})$ respectively, following the relation $[\psi_i(\vec{x}), \psi_j^\dagger(\vec{x}')] = \delta_{ij} \delta(\vec{x} - \vec{x}')$. Last term in H_0 is the two body intraspecies interaction Hamiltonian with a_i as the intraspecies s-wave scattering length of i th condensate atom having mass M . The term $\cos^2(kx) \hbar U_{0i} \hat{a}^\dagger \hat{a}$ describes the optical lattice potential experienced by each of the two species inside the cavity while V_i^{cl} is the classical potential for the two components. Here k denotes the wave vector of the pump laser field. The parameter $U_{0i} = \frac{g_{0i}^2}{\Delta_{ai}}$ is the optical lattice barrier height per photon for the i th component and it represents the atomic backaction on the field. The single atom-photon coupling strength is given by g_{0i} for the i th component while $\Delta_{ai} = \omega_p - \omega_{ai}$ is the corresponding large atom-pump detuning. Also, H_{int} depicts the inter-species two body interaction Hamiltonian where a_{12} ($= a_{21}$) is the inter-species scattering length. H_L describes the light field Hamiltonian with $\Delta_c = \omega_p - \omega_c$ representing the cavity-pump detuning and \hat{a} (\hat{a}^\dagger) to be the lowering (raising) operator such that $[\hat{a}, \hat{a}^\dagger] = 1$.

The corresponding Bose-Hubbard (BH) Hamiltonian can be derived by expanding the atomic field operators in a basis of localized Wannier functions as $\psi_1 = \sum_l \hat{b}_l W_1(\vec{x} - \vec{x}_l)$ and $\psi_2 = \sum_l \hat{c}_l W_2(\vec{x} - \vec{x}_l)$, where $W_i(\vec{x} - \vec{x}_l)$ is the Wannier function for the i th component bosonic atom at the l th site. Also, \hat{b}_l and \hat{c}_l are the annihilation operators for the 1st and 2nd component

bosonic atom respectively at the l th site. In the BH model, this substitution is valid for the lowest Bloch bands of the periodic optical lattice potential. Thus, retaining only the lowest band along with the nearest-neighbor interaction, the above Hamiltonian given by eqn. (1) becomes:

$$\begin{aligned}
 H = & E_1 \sum_l \hat{b}_l^\dagger \hat{b}_l + (\hbar U_{01} \hat{a}^\dagger \hat{a} + V_1^{cl}) J_1 \sum_l \hat{b}_l^\dagger \hat{b}_l + \frac{U_{11}}{2} \sum_l \hat{b}_l^\dagger \hat{b}_l^\dagger \hat{b}_l \hat{b}_l \\
 & + E_2 \sum_l \hat{c}_l^\dagger \hat{c}_l + (\hbar U_{02} \hat{a}^\dagger \hat{a} + V_2^{cl}) J_2 \sum_l \hat{c}_l^\dagger \hat{c}_l + \frac{U_{22}}{2} \sum_l \hat{c}_l^\dagger \hat{c}_l^\dagger \hat{c}_l \hat{c}_l \\
 & + U_{12} \sum_l \hat{b}_l^\dagger \hat{b}_l \hat{c}_l^\dagger \hat{c}_l - \hbar \Delta_c \hat{a}^\dagger \hat{a} - i \hbar \eta (\hat{a} - \hat{a}^\dagger), \tag{6}
 \end{aligned}$$

where the coupling matrix elements are:

$$E_i = \int d\vec{x} W_i(\vec{x} - \vec{x}_l) \left(\frac{-\hbar^2 \nabla^2}{2M} \right) W_i(\vec{x} - \vec{x}_l), \tag{7}$$

$$J_i = \int d\vec{x} W_i(\vec{x} - \vec{x}_l) \cos^2(kx) W_i(\vec{x} - \vec{x}_l). \tag{8}$$

Note that here we have ignored matter wave dynamics for light scattering which is justified if we consider deep lattice formed by a strong classical potential. Such a situation can easily be experimentally realized since the time scale of light measurements can be made faster than the time scale of atomic tunneling. Thus, tunneling can be made very slow by tuning the optical lattice potential [29]. Hence, tunneling of atoms into the neighbouring wells is neglected in deriving the above Hamiltonian. Also, U_{ii} and U_{12} represent the respective two body intra and inter component interaction which are defined as:

$$U_{ii} = \frac{4\pi \hbar^2 a_i}{M} \int d\vec{x} |W_i(\vec{x})|^4, \tag{9}$$

$$U_{12} = \frac{4\pi \hbar^2 a_{12}}{M} \int d\vec{x} |W_1(\vec{x})|^2 |W_2(\vec{x})|^2. \tag{10}$$

The BH Hamiltonian derived above (given by eqn. (6)) is valid for weak atom-cavity field nonlinearity only [4]. It gives the following Heisenberg-Langevin equations of motion for the photon operator \hat{a} and the bosonic field operators \hat{b}_l and \hat{c}_l :

$$\dot{\hat{a}} = -i \left\{ U_{01} J_1 \sum_l \hat{b}_l^\dagger \hat{b}_l + U_{02} J_2 \sum_l \hat{c}_l^\dagger \hat{c}_l \right\} \hat{a} + i \Delta_c \hat{a} - \frac{\kappa}{2} \hat{a} + \eta + \sqrt{\kappa} \hat{\xi}_p(t), \tag{11}$$

$$\dot{\hat{b}}_l = -i \left\{ \left(U_{01} \hat{a}^\dagger \hat{a} + \frac{V_1^{cl}}{\hbar} \right) J_1 + \frac{E_1}{\hbar} \right\} \hat{b}_l - i \frac{U_{11}}{\hbar} \hat{b}_l^\dagger \hat{b}_l \hat{b}_l - i \frac{U_{12}}{\hbar} \hat{b}_l \hat{c}_l^\dagger \hat{c}_l, \tag{12}$$

$$\dot{\hat{c}}_l = -i \left\{ \left(U_{02} \hat{a}^\dagger \hat{a} + \frac{V_2^{cl}}{\hbar} \right) J_2 + \frac{E_2}{\hbar} \right\} \hat{c}_l - i \frac{U_{22}}{\hbar} \hat{c}_l^\dagger \hat{c}_l \hat{c}_l - i \frac{U_{12}}{\hbar} \hat{c}_l \hat{b}_l^\dagger \hat{b}_l, \tag{13}$$

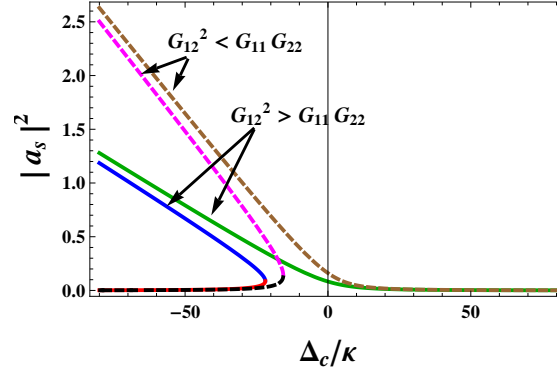


Figure 2. (color online) Plot of mean intracavity photon number $|a_s|^2$ of the pumped two-species BEC-cavity system as a function of dimensionless cavity-pump detuning Δ_c/κ for the condensates to be in the phase segregated regime ($G_{11} = 0.5\kappa$, $G_{22} = 0.75\kappa$, $G_{12} = \kappa$) (solid lines) and phase mixed regime ($G_{11} = 2.0\kappa$, $G_{22} = 3.0\kappa$, $G_{12} = \kappa$) (dashed lines). The other parameters used are $\eta^2/\kappa^2 = 10$, $U_{01} = U_{02} = -\kappa$, $J_1 = J_2 = 1$, $I = 50$, $E'_1 = E'_2 = 0$ and $V_1^{cl'} = V_2^{cl'} = -0.1\kappa$.

where κ characterizes the dissipation of the optical field. Also, $\hat{\xi}_p(t)$ is the input noise operator satisfying $\langle \hat{\xi}_p(t) \rangle = 0$, $\langle \hat{\xi}_p^\dagger(t') \hat{\xi}_p(t) \rangle = n_p \delta(t' - t)$ and $\langle \hat{\xi}_p(t') \hat{\xi}_p^\dagger(t) \rangle = (n_p + 1) \delta(t' - t)$ with n_p representing the equilibrium occupation number for the optical oscillator. The total number operator is given as $\hat{N} = \sum_l (\hat{b}_l^\dagger \hat{b}_l + \hat{c}_l^\dagger \hat{c}_l) = \hat{N}_b + \hat{N}_c$. Since we are ignoring tunneling dynamics, we drop the site index l from the atomic operators. Further note that the steady state values of the photonic operator and the atomic operators, denoted by a_s , b_s and c_s respectively (the subscript s denotes the steady-state value), can be obtained by setting the time derivatives of \hat{a} , \hat{b} and \hat{c} to zero. Thus, the resulting steady state values become:

$$|a_s|^2 = \frac{\eta^2}{\frac{\kappa^2}{4} + \{\Delta_c - U_{01}J_1I|b_s|^2 - U_{02}J_2I|c_s|^2\}^2}, \quad (14)$$

$$|b_s|^2 = \frac{1}{(G_{12}^2 - G_{11}G_{22})} \left[(U_{01}J_1G_{22} - U_{02}J_2G_{12})|a_s|^2 + (V_1^{cl'}J_1 + E'_1)G_{22} - (V_2^{cl'}J_2 + E'_2)G_{12} \right], \quad (15)$$

$$|c_s|^2 = \frac{1}{(G_{12}^2 - G_{11}G_{22})} \left[(U_{02}J_2G_{11} - U_{01}J_1G_{12})|a_s|^2 + (V_2^{cl'}J_2 + E'_2)G_{11} - (V_1^{cl'}J_1 + E'_1)G_{12} \right], \quad (16)$$

where $G_{11} = U_{11}/\hbar$, $G_{22} = U_{22}/\hbar$, $G_{12} = U_{12}/\hbar$, $V_1^{cl'} = V_1^{cl}/\hbar$, $V_2^{cl'} = V_2^{cl}/\hbar$, $E'_1 = E_1/\hbar$ and $E'_2 = E_2/\hbar$. After substituting $|b_s|^2$ and $|c_s|^2$ into the eqn. (14), we obtain a cubic equation in $|a_s|^2 (= A)$ as:

$$A^3 \delta^2 - (2\Delta'_c \delta) A^2 + \left(\frac{\kappa^2}{4} + \Delta_c'^2 \right) A - \eta^2 = 0, \quad (17)$$

where

$$\Delta'_c = \Delta_c - U_{01}J_1I \frac{\left[(V_1^{cl'}J_1 + E'_1)G_{22} - (V_2^{cl'}J_2 + E'_2)G_{12} \right]}{(G_{12}^2 - G_{11}G_{22})} - U_{02}J_2I \frac{\left[(V_2^{cl'}J_2 + E'_2)G_{11} - (V_1^{cl'}J_1 + E'_1)G_{12} \right]}{(G_{12}^2 - G_{11}G_{22})}, \quad (18)$$

$$\delta = U_{01}J_1I \frac{[(U_{01}J_1G_{22} - U_{02}J_2G_{12})]}{(G_{12}^2 - G_{11}G_{22})} + U_{02}J_2I \frac{[(U_{02}J_2G_{11} - U_{01}J_1G_{12})]}{(G_{12}^2 - G_{11}G_{22})}, \quad (19)$$

with I representing the total number of lattice sites. A plot of this algebraic equation of third order in A as a function of dimensionless cavity-pump detuning (Δ_c/κ) is shown in Figure 2 for two different conditions. When the condition $G_{12}^2 > G_{11}G_{22}$ is satisfied, then, the condensates are said to be in the phase segregated state (solid lines). However, in the opposite limit i.e., when the condition $G_{12}^2 < G_{11}G_{22}$ is satisfied, the condensates are said to be in a mixed state (dashed lines) [24]. Note that we will always work either in the deep phase mixed regime or in the deep phase segregated regime since the dynamics could be very complex at the boundary separating the two regimes [30]. Clearly, Figure 2 displays a bistable behavior. For a sufficiently large value of pump parameter η , we obtain three possible steady-state solutions for the mean intracavity photon number, with two of them being stable and one unstable [6]. In both the cases, system follows the steady-state branch until reaching the lower turning point, where non-steady-state dynamics gets excited. Here, we observe that this bistable response is very sensitive to the state we are working with. The threshold point of optical bistability in the case of phase segregated state appears at a smaller value of detuning as compared to the case of the phase mixed state. Therefore, we need to choose the appropriate value of cavity-pump detuning depending on the regime we are working with. Thus, cavity-pump detuning plays a very significant role in controlling the bistability in the system. Further note that the contrast between the highest and the lowest stable steady-state values gets decreased for the condensates in the phase segregated regime. So, the optical bistability threshold point in the phase segregated state can be achieved at a lower detuning at the cost of lower contrast between the highest and lowest stable mean-field solutions. Hence, both the threshold point and contrast between the bistability values can be controlled depending upon our interest of working in either of the regimes. Now, in the next section, we study the dynamics of fluctuations of the system around the steady state values in both the phase mixed and phase segregated regimes.

3. Fluctuation Dynamics: Normal-Mode Splitting

In this section, we show that the coupling of the cavity field fluctuations and the fluctuations of the two condensate components leads to the splitting of normal mode into three modes, known as normal-mode splitting (NMS). This NMS involves driving three parametrically coupled non-degenerate modes out of equilibrium. The aim would be to study the influence of phase mixing and phase segregation on NMS. To this end, we linearize eqns. (11)-(13) around the steady-state values by writing operators as the sum of averages plus fluctuations (i.e., $\hat{a} \rightarrow a_s + \hat{a}$, $\hat{b} \rightarrow \sqrt{n_{bs}} + \hat{b}$ and $\hat{c} \rightarrow \sqrt{n_{cs}} + \hat{c}$ with $\sqrt{n_{bs}} = \sqrt{\frac{N_b}{I}}$ and $\sqrt{n_{cs}} = \sqrt{\frac{N_c}{I}}$) in order to obtain the following Heisenberg-Langevin equations of motion:

$$\dot{\hat{a}} = \left[i\Delta_d - \frac{\kappa}{2} \right] \hat{a} - i\bar{U}_{01}I(\hat{b} + \hat{b}^\dagger) - i\bar{U}_{02}I(\hat{c} + \hat{c}^\dagger) + \sqrt{\kappa}\hat{\xi}_p(t), \quad (20)$$

$$\dot{\hat{b}} = -iv_b\hat{b} - i\bar{U}_{11}\hat{b}^\dagger - i\bar{U}_{12}(\hat{c} + \hat{c}^\dagger) - i\bar{U}_{01}(\hat{a} + \hat{a}^\dagger), \quad (21)$$

$$\dot{\hat{c}} = -iv_c\hat{c} - i\bar{U}_{22}\hat{c}^\dagger - i\bar{U}_{12}(\hat{b} + \hat{b}^\dagger) - i\bar{U}_{02}(\hat{a} + \hat{a}^\dagger). \quad (22)$$

Here, $\nu_b = U_{01}J_1|a_s|^2 + V_1^{cl'}J_1 + E'_1 + 2G_{11}n_{bs} + G_{12}n_{cs}$, $\bar{U}_{11} = G_{11}n_{bs}$, $\bar{U}_{12} = G_{12}\sqrt{n_{bs}}\sqrt{n_{cs}}$, $\bar{U}_{01} = U_{01}J_1|a_s|\sqrt{n_{bs}}$, $\nu_c = U_{02}J_2|a_s|^2 + V_2^{cl'}J_2 + E'_2 + 2G_{22}n_{cs} + G_{12}n_{bs}$, $\bar{U}_{22} = G_{22}n_{cs}$, $\bar{U}_{02} = U_{02}J_2|a_s|\sqrt{n_{cs}}$ and $\Delta_d = \Delta_c - U_{01}J_1In_{bs} - U_{02}J_2In_{cs}$. The atomic losses due to heating are neglected. Now, we rewrite the above equations of motion in terms of amplitude and phase quadratures for the system with $X_a = \hat{a} + \hat{a}^\dagger$, $X_b = \hat{b} + \hat{b}^\dagger$, $X_c = \hat{c} + \hat{c}^\dagger$, $P_a = i(\hat{a}^\dagger - \hat{a})$, $P_b = i(\hat{b}^\dagger - \hat{b})$, $P_c = i(\hat{c}^\dagger - \hat{c})$, $X_a^{in}(t) = (\hat{\xi}_p(t) + \hat{\xi}_p^\dagger(t))$ and $P_a^{in}(t) = i(\hat{\xi}_p^\dagger(t) - \hat{\xi}_p(t))$ as:

$$\dot{X}_a = -\frac{\kappa}{2}X_a - \Delta_d P_a + \sqrt{\kappa}X_a^{in}(t), \quad (23)$$

$$\dot{P}_a = -\frac{\kappa}{2}P_a + \Delta_d X_a - 2\bar{U}_{01}IX_b - 2\bar{U}_{02}IX_c + \sqrt{\kappa}P_a^{in}(t), \quad (24)$$

$$\dot{X}_b = (\nu_b - \bar{U}_{11})P_b, \quad (25)$$

$$\dot{P}_b = -(\nu_b + \bar{U}_{11})X_b - 2\bar{U}_{12}X_c - 2\bar{U}_{01}X_a, \quad (26)$$

$$\dot{X}_c = (\nu_c - \bar{U}_{22})P_c, \quad (27)$$

$$\dot{P}_c = -(\nu_c + \bar{U}_{22})X_c - 2\bar{U}_{12}X_b - 2\bar{U}_{02}X_a. \quad (28)$$

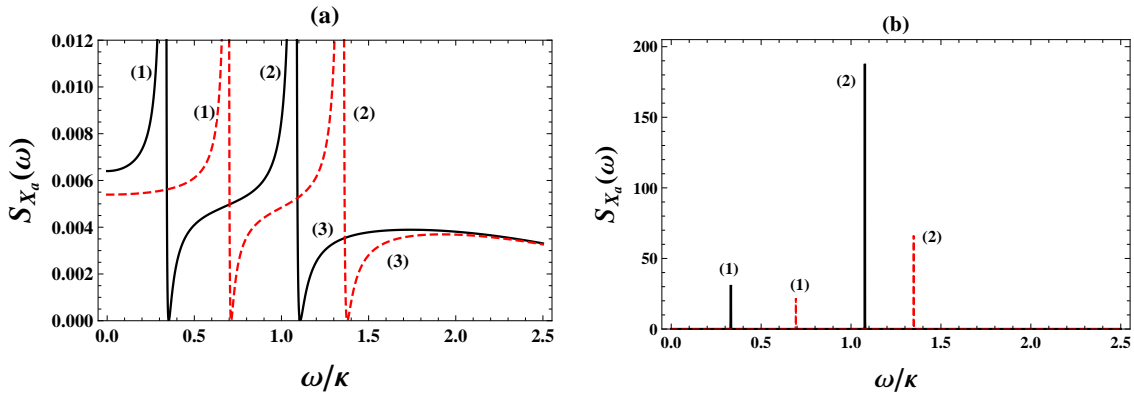


Figure 3. (color online) (a) Plot of the output cavity spectrum $S_{X_a}(\omega)$ as a function of normalized frequency ω/κ for the condensates to be in the phase segregated regime ($G_{11} = 0.8\kappa$, $G_{22} = 0.75\kappa$, $G_{12} = \kappa$) (solid line) and phase mixed regime ($G_{11} = 1.05\kappa$, $G_{22} = 1.15\kappa$, $G_{12} = \kappa$) (dashed line). (b) same plot as (a) but including higher ordinate as well. The other parameters used are $U_{01} = 1.2\kappa$, $U_{02} = 0.2\kappa$, $J_1 = J_2 = 1$, $I = 20$, $E'_1 = E'_2 = 0$, $V_1^{cl'} = -0.3\kappa$, $V_2^{cl'} = -0.5\kappa$, $\Delta_c = -\kappa$ and $n_{bs} = n_{cs} = 0.5$.

Note that the system reaches a steady state only if it is stable. Therefore, the stability conditions given in Appendix A is always satisfied here for the system to be in the stable regime. Furthermore, the output cavity spectrum in the Fourier space for $n_p = 0$ can be evaluated from:

$$S_{X_a}(\omega) = \frac{1}{4\pi} \int d\omega' e^{-i(\omega+\omega')t} \langle X_a(\omega)X_a(\omega') + X_a(\omega')X_a(\omega) \rangle, \quad (29)$$

using the correlations given in Appendix B and is found to be:

$$S_{X_a}(\omega) = \frac{\kappa\Delta_1^2 \left[\Delta_d^2 + \frac{\kappa^2}{4} + \omega^2 \right]}{\left[\left\{ \Delta_1 \left(\frac{\kappa^2}{4} - \omega^2 \right)^2 + \Delta_2\Delta_d \right\}^2 + \omega^2\kappa^2\Delta_1^2 \right]}, \quad (30)$$

where

$$\Delta_1 = (\omega^2 - v_b^2 + \bar{U}_{11}^2)(\omega^2 - v_c^2 + \bar{U}_{22}^2) - 4\bar{U}_{12}^2(v_b - \bar{U}_{11})(v_c - \bar{U}_{22}), \quad (31)$$

$$\begin{aligned} \Delta_2 = \Delta_d \Delta_1 - 16I\bar{U}_{01}\bar{U}_{02}\bar{U}_{12}(v_b - \bar{U}_{11})(v_c - \bar{U}_{22}) - 4\bar{U}_{01}^2 I(v_b - \bar{U}_{11})(\omega^2 - v_c^2 + \bar{U}_{22}^2) \\ - 4\bar{U}_{02}^2 I(v_c - \bar{U}_{22})(\omega^2 - v_b^2 + \bar{U}_{11}^2). \end{aligned} \quad (32)$$

The optical spectrum is driven by the quantum fluctuations of the condensates. As before, we are interested either in the deep phase mixed state or in the deep phase segregated state. Figure 3(a) shows the plot of displacement spectrum $S_{X_a}(\omega)$ versus normalized frequency (ω/κ) for the condensates to be in the phase segregated regime $G_{12}^2 > G_{11}G_{22}$ (solid line) and phase mixed regime $G_{12}^2 < G_{11}G_{22}$ (dashed line). Here, we demonstrate the splitting of normal mode into three modes for both the cases, which is clearly indicated by the presence of three distinct peaks in the optical spectra. The NMS is basically associated with the mixing between the fluctuations of cavity field mode around the steady state and the fluctuations of two component condensates (Bogoliubov modes) around the mean field. Therefore, the presence of three peaks in the spectra indicates a coherent energy exchange between the optical mode and the two Bogoliubov modes. Note that the energy exchange between these modes should take place on a time scale faster than the decoherence of each of the modes, otherwise NMS would not be observed. Furthermore, an important point to note from Figure 3(a) is the shifting of peaks towards higher frequencies as we move from segregated to mixed state. Also, from figure 3(b) (which depicts the same plot of Figure 3(a) but including higher ordinate as well), amplitude discrepancies are also observed. In phase mixed case, amplitude of all the three peaks are found to be comparatively smaller than the phase segregated case. Thus, along with the observation of NMS in both the spectra, discrepancies in the position and amplitude of the peaks are also clearly demonstrated in both the cases.

Further note that the parameters considered here are in the range of experimental capabilities. A high-finesse optical cavity consisting of a cloud of BEC may have the intracavity decay rate varying from $2\pi \times 8.75\text{kHz}$ [31], to $2\pi \times 0.66\text{MHz}$ [32] or $2\pi \times 1.3\text{MHz}$ [6]. Thus, the value of pump amplitude η chosen here for optical bistability is experimentally reachable [6, 33]. The other parameters taken in the units of cavity damping rate are also within the experimental reach [34]. Further, the values for the intraspecies and interspecies interaction between the condensate atoms are chosen in such a way that the conditions for the condensates to be either in the phase mixed state or in the phase segregated state are satisfied [30].

4. Conclusion

To summarize, we have theoretically demonstrated the possibility of observing optical bistability and normal mode splitting for a weakly interacting two-species Bose-Einstein condensates confined within an optical cavity for two different regimes – the phase mixed regime and the phase segregated regime. We found that the optical bistability threshold point and the contrast between the bistability values are very sensitive to the state we are working with. In particular, the threshold point in the phase segregated state can be achieved at a lower value of cavity-pump detuning at the cost of lower contrast between the bistability values. Thus, an

appropriate value of cavity-pump detuning is to be chosen depending upon our interest of the state to work in. Such system may be useful in making photonic switching devices. Furthermore, in the optical spectrum, along with the normal mode splitting into three modes (optical mode and two Bogoliubov modes), discrepancies in the amplitude position and peaks have also been clearly observed in both the regimes. In the phase mixed state, smaller amplitude peaks shifting towards larger frequencies have been accounted comparative to the phase segregated case.

Appendix A

The two non-trivial stability conditions for the system, attained by applying the Routh-Hurwitz criterion [35, 36], are given as:

$$S_1 = a_0 > 0, \quad (\text{A.1})$$

$$S_2 = (a_5 a_4 a_3 + a_6 a_1 a_5 - a_6 a_3^2 - a_2 a_5^2) > 0, \quad (\text{A.2})$$

where

$$\begin{aligned} a_0 = & \frac{\kappa^2}{4} [v_b^2 v_c^2 - v_b^2 \bar{U}_{22}^2 - v_c^2 \bar{U}_{11}^2 + \bar{U}_{11}^2 \bar{U}_{22}^2 - 4\bar{U}_{12}^2 (v_b v_c - v_b \bar{U}_{22} - v_c \bar{U}_{11} + \bar{U}_{11} \bar{U}_{22})] \\ & + (v_b - \bar{U}_{11})(4I\Delta_d \bar{U}_{01}^2 v_c^2 - 4I\Delta_d \bar{U}_{01}^2 \bar{U}_{22}^2) + 4I\Delta_d \bar{U}_{02}^2 (v_b^2 - \bar{U}_{11}^2)(v_c - \bar{U}_{22}) \\ & + \Delta_d^2 [\bar{U}_{11}^2 \bar{U}_{22}^2 - 4\bar{U}_{11} \bar{U}_{22} \bar{U}_{12}^2 + 4\bar{U}_{22} v_b \bar{U}_{12}^2 - \bar{U}_{22}^2 v_b^2 + 4\bar{U}_{11} v_c \bar{U}_{12}^2 - 4v_b v_c \bar{U}_{12}^2 - \bar{U}_{11}^2 v_c^2 + v_b^2 v_c^2] \\ & - 16\bar{U}_{01} \bar{U}_{02} \bar{U}_{12} I\Delta_d (v_c v_b - v_c \bar{U}_{11} - v_b \bar{U}_{22} + \bar{U}_{11} \bar{U}_{22}), \end{aligned} \quad (\text{A.3})$$

$$a_1 = \kappa [v_b^2 v_c^2 - v_b^2 \bar{U}_{22}^2 - v_c^2 \bar{U}_{11}^2 + \bar{U}_{11}^2 \bar{U}_{22}^2 - 4\bar{U}_{12}^2 (v_b v_c - v_b \bar{U}_{22} - v_c \bar{U}_{11} + \bar{U}_{11} \bar{U}_{22})], \quad (\text{A.4})$$

$$\begin{aligned} a_2 = & \frac{\kappa^2}{4} [v_b^2 + v_c^2 - \bar{U}_{11}^2 - \bar{U}_{22}^2] + v_b^2 v_c^2 - v_b^2 \bar{U}_{22}^2 - v_c^2 \bar{U}_{11}^2 + \bar{U}_{11}^2 \bar{U}_{22}^2 \\ & - 4\bar{U}_{12}^2 [v_b v_c - v_b \bar{U}_{22} - v_c \bar{U}_{11} + \bar{U}_{11} \bar{U}_{22}] + 4I\Delta_d \bar{U}_{01}^2 (v_b - \bar{U}_{11}) + 4I\Delta_d \bar{U}_{02}^2 (v_c - \bar{U}_{22}) \\ & + \Delta_d^2 [v_b^2 + v_c^2 - \bar{U}_{11}^2 - \bar{U}_{22}^2], \end{aligned} \quad (\text{A.5})$$

$$a_3 = \kappa [v_b^2 + v_c^2 - \bar{U}_{11}^2 - \bar{U}_{22}^2], \quad (\text{A.6})$$

$$a_4 = \frac{\kappa^2}{4} + \Delta_d^2 - \bar{U}_{11}^2 - \bar{U}_{22}^2 + v_b^2 + v_c^2, \quad (\text{A.7})$$

$$a_5 = \kappa, \quad (\text{A.8})$$

$$a_6 = 1. \quad (\text{A.9})$$

Appendix B

The amplitude and phase quadratures of the input noise operator in the Fourier space satisfy the following correlation functions [37]:

$$\langle X_a^{in}(\omega) X_a^{in}(\omega') \rangle = \langle P_a^{in}(\omega) P_a^{in}(\omega') \rangle = 2\pi \delta(\omega + \omega'), \quad (\text{B.1})$$

$$\langle X_a^{in}(\omega)P_a^{in}(\omega') \rangle = 2i\pi\delta(\omega + \omega'), \quad (\text{B.2})$$

$$\langle P_a^{in}(\omega)X_a^{in}(\omega') \rangle = -2i\pi\delta(\omega + \omega'). \quad (\text{B.3})$$

Competing Interests

The authors declare that they have no competing interests.

Authors' Contributions

All the authors contributed equally and significantly in writing this article. All the authors read and approved the final manuscript.

References

- [1] S. Gupta, K.L. Moore, K.W. Murch and D.M. Stamper-Kurn, *Phys. Rev. Lett.* **99** (2007), 213601.
- [2] P. Domokos and H. Ritsch, *Phys. Rev. Lett.* **89** (2002), 253003.
- [3] S. Slama et al., *Phys. Rev. Lett.* **98** (2007), 053603.
- [4] J. Larson, B. Damski, G. Morigi and M. Lewenstein, *Phys. Rev. Lett.* **100** (2008), 050401.
- [5] K. Baumann, C. Guerlin, F. Brennecke and T. Esslinger, *Nature* **464** (2010), 1301.
- [6] F. Brennecke, S. Ritter, T. Donner and T. Esslinger, *Science* **322** (2008), 235.
- [7] H.M. Gibbs, *Controlling Light with Light* (Orlando: Academic, 1985).
- [8] A. Joshi and M. Xiao, *Phys. Rev. Lett.* **91** (2003), 143904.
- [9] H. Chang, H. Wu, C D. Xie and H. Wang, *Phys. Rev. Lett.* **93** (2004), 213901.
- [10] L. Zhou, H. Pu, H.Y. Ling and W. Zhang, *Phys. Rev. Lett.* **103** (2009), 160403.
- [11] S. Yang, M. Al-Amri, J. Evers and M.S. Zubairy, *Phys. Rev. A* **83** (2011), 053821.
- [12] C.J. Myatt et al., *Phys. Rev. Lett.* **78** (4) (1997), 586.
- [13] S.B. Papp, J.M. Pino and C.E. Wieman, *Phys. Rev. Lett.* **101** (4) (2008), 040402.
- [14] G. Ferrari et al., *Phys. Rev. Lett.* **89** (5) (2002), 053202.
- [15] G. Modugno et al., *Phys. Rev. Lett.* **89** (19) (2002), 190404.
- [16] G. Thalhammer et al., *Phys. Rev. Lett.* **100** (21) (2008), 210402.
- [17] D.J. McCarron et al., *Phys. Rev. A* **84** (1) (2011), 011603.
- [18] D.S. Hall et al., *Phys. Rev. Lett.* **81** (1998), 1539.
- [19] P. Maddaloni et al., *Phys. Rev. Lett.* **85** (2000), 2413.
- [20] G. Delannoy et al., *Phys. Rev. A* **63** (2001), 051602.
- [21] K. M. Mertes et al., *Phys. Rev. Lett.* **99** (2007), 190402.
- [22] R.P. Anderson, C. Ticknor, A.I. Sidorov and B.V. Hall, *Phys. Rev. A* **80** (2009), 023603.
- [23] S. Tojo et al., *Phys. Rev. A* **82** (2010), 033609.
- [24] C.J. Pethick and H. Smith, *Bose-Einstein Condensation in Dilute Gases*, Cambridge University Press, Cambridge (2002).

- [25] S. Inouye et al., *Nature* **392** (1998), 151.
- [26] P. Ao, S. T. Chui, *Phys. Rev. A* **58** (1998), 4836.
- [27] P. Ao and S.T. Chui, *J. Phys. B: At. Mol. Opt. Phys.* **33** (2000), 535.
- [28] A. Bhattacharjee, *J. Phys. B: At. Mol. Opt. Phys.* **43** (2010), 205301.
- [29] D. Jaksch et al., *Phys. Rev. Lett.* **81** (1998), 3108.
- [30] A.B. Bhattacharjee, *Phys. Scr.* **78** (2008), 045009.
- [31] B. Nagorny et al., *Phys. Rev. A* **67** (2003), 031401.
- [32] K.W. Murch et al., *Nature Phys.* **4** (2008), 561.
- [33] S. Ritter et al., *Appl. Phys. B* **95** (2009), 213.
- [34] C. Maschler and H. Ritsch, *Phys. Rev. Lett.* **95** (2005), 260401.
- [35] I.S. Gradshteyn and I.M. Ryzhik, *Table of Integrals, Series and Products*, Academic Press, Orlando, FL (1980), p. 1119.
- [36] E.X. DeJesus and C. Kaufman, *Phys. Rev. A* **35** (1987), 5288.
- [37] V. Giovannetti, P. Tombesi and D. Vitali, *Phys. Rev. A* **63** (2001), 023812.